Machine Learning based Analysis of RVE in Concrete Structures

Saulo S. de Castro[1],José David S. S. M. Almeida[1], Hugo M. Leão[1], Roque L. S. Pitangueira[1]

[1]*Dept. of Structures Engineering, Federal University of Minas Gerais*
Av. Antonio Carlos, 6627, Pampulha, Belo Horizonte, 31270-901, Minas Gerais, Brazil
saullo9@yahoo.com.br,jose.david.ssma@gmail.com, hugomleao@yahoo.com.br, roque@dees.ufmg.com

Abstract. In the numerical modeling of structural elements, particularly utilizing the finite element method (FEM), multiscale models represent the most robust approach for analyzing heterogeneous materials such as concrete. These models incorporate information from multiple scales—typically, macroscopic and mesoscopic—to more accurately capture the material's response and its impact on structural behavior. In this context, each material point in the numerical model is associated with a Representative Volume Element (RVE), which is the smallest statistically representative portion of the material. During the analysis of a multiscale model via FEM, each integration point in the model requires the execution of an independent computational model that simulates the RVE and is processed in parallel to the main model (on the fly process). Deformations originating from the macroscale are applied to the mesoscale models, and the responses obtained are then reintegrated into the macroscale. This approach results in significant demand on processing resources and time, which can limit its practical application in large-scale projects or situations requiring rapid responses. This article propose the representation of the RVE through a Machine Learning model (ML) capable of simulating the mechanical behavior of the material. This approach eliminates the on the fly processing. Throughout the text, examples of RVEs represented by ML models are presented, and their specificities are discussed. Finally, the advantages and disadvantages of this methodology are examined.

Keywords: Multiscale Models, Machine Learning, RVE.

1 Introduction

Numerical modeling of structural elements using the Finite Element Method (FEM) is extensively employed in civil engineering, particularly for the analysis of heterogeneous materials such as concrete. In practical applications, models at a single scale are commonly utilized to represent concrete, often employing linear elastic models with modifications to approximately capture the material's physical nonlinearities. This approach predominates due to the challenges associated with applying constitutive models at scales that can accurately represent the nonlinear behavior of concrete, especially due to the complexity of obtaining the necessary parameters for these models. In this context, more advanced models, such as those based on damage mechanics or phase field theory, are seldom applied in practice.

Due to the nature of concrete, a more appropriate numerical representation would be through multiscale models, which integrate information at both the macroscopic and mesoscopic scales. This advanced methodology allows for a more accurate simulation of mechanical properties and structural behavior, providing crucial insights for failure prediction and the more efficient design of structures. However, the implementation of multiscale models in FEM faces significant challenges, particularly in terms of computational demand. Each integration point in the model requires the parallel execution of an independent computational model to simulate the Representative Volume Element (RVE). This process, known as "on the fly," is essential to ensure result accuracy but significantly increases the use of computational resources and the time required to complete analyses. This characteristic may limit the technique's applicability in large-scale projects or situations requiring quick and efficient responses, making multiscale models an even more distant reality from practical applications compared to single-scale nonlinear models.

To overcome these challenges, it is ideal to develop a multiscale model that utilizes an RVE driven by simple parameters. This model should employ, for each constituent of the RVE, constitutive models at a scale capable of capturing the nonlinearities of the constituent, but driven by simple and practical parameters. Furthermore, the models representing the RVEs should have a very low computational cost, enabling their application in analyses

of structural elements with dimensions typical of practical applications. To develop a model with these characteristics, the authors propose representing the RVE through a Machine Learning (ML) model capable of simulating the mechanical behavior of the material, thus eliminating the need for on-the-fly processing. Additionally, it is proposed that the RVE be characterized by simple and accessible parameters in practical contexts. Throughout the text, the methodology developed to achieve this objective, examples of RVEs represented by ML models, and their specificities are discussed. Finally, the advantages and disadvantages of this methodology are examined.

2 Theoretical Principles

2.1 RVE Definition

Multiscale methods have achieved success largely due to the selection and identification of a Representative Volume Element (RVE) with suitable dimensions. Trusov and Keller [1] define the RVE as the smallest volume of material that encompasses a statistically adequate number of deformation mechanisms. Expanding this volume should not alter the evolution equations governing the field variables associated with these mechanisms. Different researchers have proposed various definitions of the RVE, all of which share the common objective of ensuring that the RVE is sufficiently small compared to the macroscale structural dimensions, yet large enough to represent the material's microstructure and encompass all mechanisms responsible for its physical non-linearities [2]. The concern about the small size of the RVE relative to the problem's dimension is to ensure that its representativeness is unaffected by the boundary conditions at the macroscale [3]. Furthermore, accurately defining the RVE necessitates a clear distinction between observation scales. Additionally, the RVE should demonstrate homogeneity and ergodicity [3]. It is crucial to note that ergodic properties are essential for the RVE to ensure that its average characteristics match those of the entire material when observed at different locations. This is vital because it guarantees that the RVE's behavior statistically represents the material's overall behavior, enabling accurate and consistent analysis of properties and physical phenomena, regardless of the specific location within the material.

Determining the size of a Representative Volume Element (RVE) lacks a standardized approach [2]. Various methodologies have been proposed and implemented to quantify the dimensions of RVEs. However, comparing RVE sizes remains challenging due to differences (i) across various stages of loading, (ii) between materials with distinct properties, and (iii) under different testing conditions.

In efforts to determine the size of the representative volume element (RVE), numerous researchers have sought to establish a correlation between RVE size and the maximum dimension of inclusions [2]. For concrete, specifically, Van Mier and van Vliet [4] propose that the RVE should be approximately 3-5 times the size of the largest inclusion. Bazan, on the other hand, suggested a specific volume for the RVE, denoted as [5].

While certain studies focus on the correlation between RVE size and inclusion dimensions, others explore alternative approaches to determine RVE dimensions [2]. These approaches consider factors such as the volumetric fraction of inclusions, variations in stiffness between inclusions and the matrix, and the particle size distribution of the material. This method typically involves more advanced techniques and a greater reliance on statistical analyses.

In the present study, to determine the appropriate size of the RVE, a series of numerical simulations was performed to evaluate the mechanical behavior of various RVEs, with sizes being multiples of the maximum aggregate diameter (D_{max}). These simulations produced homogenized stress-strain curves for each RVE. The criterion for determining the optimal RVE size is based on the convergence of these curves: two consecutive RVE sizes are identified whose curves show minimal deviation. The RVE size is then selected as the smaller of these two values, ensuring an adequate representation of macroscopic properties with the smallest possible volume. Following this methodology, the RVE was assumed to be $2.5D_{\text{max}}$, a value consistent with the limits established by Van Mier and van Vliet [4]. Further details on the methodology for determining the RVE size are beyond the scope of this work and can be found in.

2.2 Phase-field theory applied to constitutive models.

Phase field models are mathematical and computational techniques that describe the crack evolution by utilizing continuous field variables to represent the state of the material. These models enable the capture of the smooth transition between intact and damaged phases, facilitating the accurate simulation of crack initiation, propagation, and merging without the necessity for explicit tracking of fracture surfaces.

The development of these models is grounded in the variational approach to Griffith's classical energy balance for brittle fractures. In this context, the energy balance of a deformable body Ω containing a crack on surface S is variationally expressed as follows [6]:

$$\Pi = \int_{\Omega} \psi(u) \ d\Omega + \int_{s} G_c \ dS. \tag{1}$$

where $\psi(u)$ is the elastic strain energy density as a function of displacement, and G_c is the critical energy release rate characterizing the fracture resistance of the material.

Minimizing eq.1 is mathematically infeasible due to the indeterminate nature of S. To address this challenge, regularization of the fracture topology is introduced, conceptualizing it as a zone of diffuse damage. In this formulation, material damage is quantified by a variable, ϕ, ranging from 0 (undamaged material) to 1 (completely damaged material). Consequently, the model does not represent the formation of discrete cracks as occurs in Griffith's theory; instead, it represents the propagation of fractures through a region with a smears damaged. This approach leads to a model capable of managing topologically complex fractures, which is crucial for accurately representing the degradation of quasi-brittle materials such as concrete. This capability was a key factor in the model's selection for this study. Consequently, eq.1 can be approximated as shown in [7, 8].

$$\Pi = \int_{\Omega} \underbrace{(1-\phi)^2}_{g(\phi)} \psi(u) \ d\Omega + \int_{\Omega} G_c \underbrace{\frac{1}{2l_0}\phi^2 + \frac{l_0}{2} \mid \nabla\phi \mid^2}_{\Gamma_c(\phi,\nabla\phi)} \ d\Omega. \tag{2}$$

In this context, $g(\phi)$ is defined as a continuous degradation function that progressively reduces the material's stiffness as the phase-field approaches the crack state ($\phi = 1$). The term $\Gamma_c(\phi, \nabla\phi)$ represents the crack density functional, which facilitates the tracking of the evolving crack surface S. Several forms for the function $g(\phi)$ have been suggested in the literature [7, 9, 10]; in this study, the formulation proposed by [7] has been utilized. Similarly, various crack density functionals have been introduced [11–13], and in this work, the approach described in [7] has been adopted.

It is important to recognize that the crack density functional depends on the parameter l_0, which serves as a prescribed length scale parameter that controls the extent of fracture regularization. Some researchers interpret this parameter as a purely mathematical tool intended to represent Griffith's fracture theory within a diffuse, continuous zone, such that the phase-field solution should converge to a discrete fracture solution as l_0 approaches zero [14, 15]. Additionally, other researchers propose that l_0 signifies a specific material property closely linked to the critical stress necessary for fracture initiation [14, 15].

Based on Eq.2, the macroscopic equilibrium condition and the evolution equations for the phase-field can be derived, resulting in an interaction between the displacement field (u) and the phase field (ϕ).

$$\begin{aligned} \sigma_{ij,i}(u,\phi) + b_i &= 0 \\ G_c\left(\frac{\phi}{l_0} - \nabla^2\phi\right) - 2(1-\phi)\psi(u) &= 0 \end{aligned} \tag{3}$$

where b_i is the body force term, with the Cauchy stress, σ_{ij}, related to the elastic strain, ε_{ij}, and the fourth-order elasticity (stiffness) tensor, C_{ijkl}, by

$$\sigma_{ij} = \frac{\partial \Pi}{\partial \varepsilon_{ij}} = g(\phi) C_{ijkl} \varepsilon_{kl} \tag{4}$$

The weak formulation of equation 3 facilitates the discretization of (u, ϕ) through a standard finite element method, allowing for the computation of the residual and stiffness matrices. The details of this numerical implementation are thoroughly discussed in [16].

It is important to note that l_0 was initially introduced (equation 2) as a mathematical tool to transform a discrete crack surface into a smooth, continuous gradient, thereby representing a diffuse crack. Additionally, it indirectly influences the element size within a finite element mesh, since excessively large elements may result in models that inadequately capture the dynamics of damage evolution, leading to inaccuracies. Therefore, phase field models used in the simulation of RVEs require highly refined meshes, particularly when the RVEs account for the presence of an ITZ. As a result, the computational expense of these models is considerable, motivating research into alternative approaches for RVE simulations.

2.3 Machine Learning models

Machine Learning, as initially described by Samuel in the late 1950s [17], entails the creation of algorithms that enable computers to learn from data autonomously, without direct programming. In contemporary contexts, ML is acknowledged as a branch of artificial intelligence dedicated to developing algorithms that detect patterns in data, facilitating generalization and high-precision prediction of future events. This ability renders ML particularly effective in addressing complex problems that traditional approaches struggle to solve [18–21].

This research concentrated on Supervised Learning Algorithms, which necessitate labeled training data to learn specific tasks. These algorithms evaluate input features (attributes) to predict target values (labels) by estimating the likelihood of the label given the features. The study investigated the feasibility of using Artificial Neural Networks (ANNs) to predict the Phase Field in a numerical simulation, which is succinctly discussed.

Artificial Neural Networks are computational frameworks modeled after the central nervous system of living organisms. They consist of numerous basic processing units, referred to as neurons, that operate concurrently to store and apply knowledge. ANNs are proficient in pattern recognition, making them applicable to both classification and regression tasks. The conceptual structure of an artificial neuron parallels that of a biological neuron.

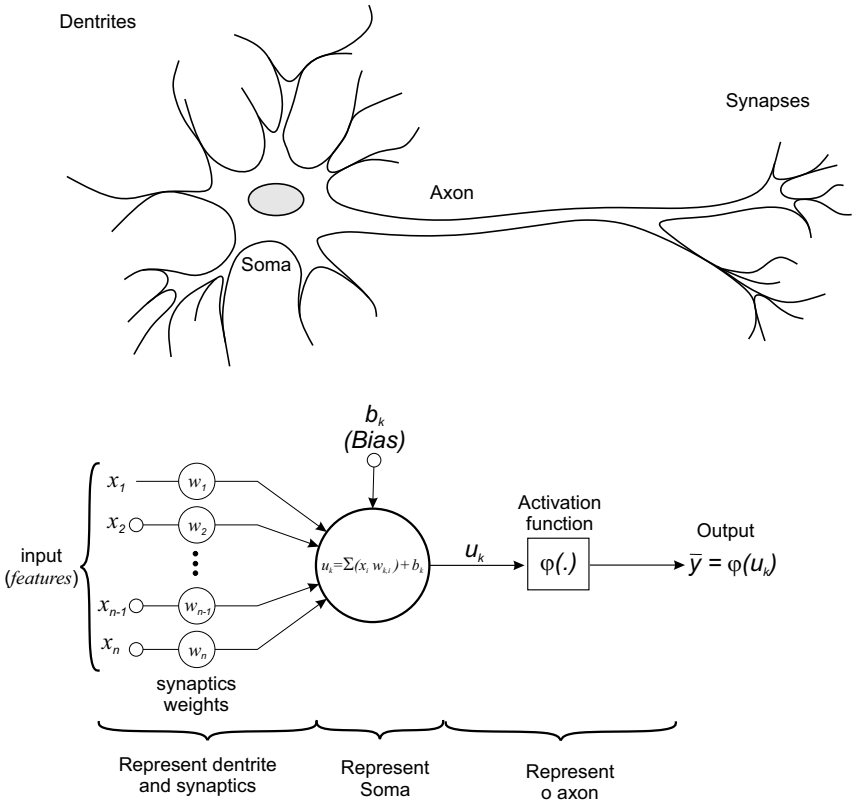

Figure 1. Idealization of the first artificial neuron proposed by [22]

An artificial neuron receives input signals, each modulated by a synaptic weight. The neuron's activity is computed as the weighted sum of these inputs, supplemented by a bias. The output of the neuron is determined by applying an activation function to this activity. Synaptic weights are generally initialized randomly and are adjusted during training to reduce the error, which is quantified by a cost function. This adjustment is critical to optimizing the model's predictive accuracy. The Perceptron, the most elementary form of an artificial neuron, was first proposed by Rosenblatt in 1958 [23] and remains a cornerstone in modern neural network architecture.

A neural network typically comprises multiple layers of artificial neurons, including an input layer, one or more hidden layers, and an output layer. The input layer captures the features representing the problem, while the output layer generates the network's predictions. Hidden layers, which can vary in number and neuron density, process information between these layers. In densely connected layers, each neuron in one layer is linked to every neuron in the next layer.

The Backpropagation algorithm, introduced by Rumelhart and collaborators in 1986 [24], is a crucial training technique for Multilayer Perceptrons (MLPs), a prevalent type of ANN. Although not the sole training algorithm, Backpropagation is fundamental and has significantly influenced numerous algorithms developed subsequently for training ANNs [18–21].

3 Methodology

As discussed in Section 1, the aim of this study is to explore the practical feasibility of multiscale models through machine learning (ML) techniques. The initial step involves proposing the use of ML models to represent an RVE. For this purpose, a Multilayer Perceptron Neural Network (MLP) was trained to simulate the mechanical behavior of an RVE under uniaxial tension.

The training of the MLP was based on a dataset composed of responses from various numerical simulations representing different RVEs. In all simulations, a fixed size of $2.5D_{max}$ was used, where D_{max} denotes the maximum aggregate diameter. The simulations followed the granulometric curves recommended by ABNT NBR 7211:2005, using the three curves with the smallest granulometry typical of conventional concretes, classified from the finest to the coarsest and sequentially named A, B, and C. Three aggregate fractions were considered: 20%, 30%, and 40%.

To randomly distribute the aggregates within an RVE, the "take and place" algorithm proposed by [25] was employed. For each aggregate fraction and granulometric curve, five simulations were conducted, each with a distinct random grain distribution. The number of five simulations was determined as the minimum required to ensure a stable average behavior. Each simulated RVE generated a stress-strain curve, obtained by homogenizing the stresses and strains within the element domain. These curves will form the training data for the ML model.

The numerical models (used to generate the training data) utilized the isotropic phase-field constitutive model proposed by [author], with the following properties for the mortar matrix: Young's modulus $E = 21876.0\,\text{kN/mm}^2$, Poisson's ratio $\nu = 0.18$, critical energy release rate $G_c = 1.8\times10^{-2}\,\text{kN/mm}$, and scale parameter $l_0 = 2.234\,\text{mm}$. For the aggregates, the following properties were used: Young's modulus $E = 100000\,\text{kN/mm}^2$, Poisson's ratio $\nu = 0.2$, critical energy release rate $G_c = 13 \times 10^{-2}\,\text{kN/mm}$, and scale parameter $l_0 = 2.234\,\text{mm}$. A transition interface was not considered in the simulations.

A multi-layer perceptron (MLP) model with two hidden layers, comprising 100 and 100 neurons, respectively, was developed. The ReLU activation function was employed in the hidden layers, and the identity function was used in the output layer. The model was trained over 50 epochs using the Adam optimization algorithm with a learning rate of 0.001. Implementation was carried out using the Scikit-learn library.

As input variables, the identification of the grain size distribution curve, the aggregate fraction, the current state of strain, and the deformation increments were considered. With significant value, the ML model predicted the corresponding state of stress.

This methodology generated a database containing 131,752 examples, all of which were utilized for training the ML model. To validate the model, an additional database was created, consisting of the averages of responses from each group of RVE corresponding to a specific particle size distribution curve with a given aggregate fraction. The use of these average curves aims to assess the model's proximity to the average behavior of the RVE used in training. Additionally, the model's results were compared to the average response of five RVE corresponding to curve A and an aggregate fraction of 0.27. This particular RVE represents a type entirely distinct from those used in the model training.

In the following section, the results obtained up to the current stage of the research are presented.

4 Results

The computational results of validation test are presented in Figure 2 and Figure 3 .

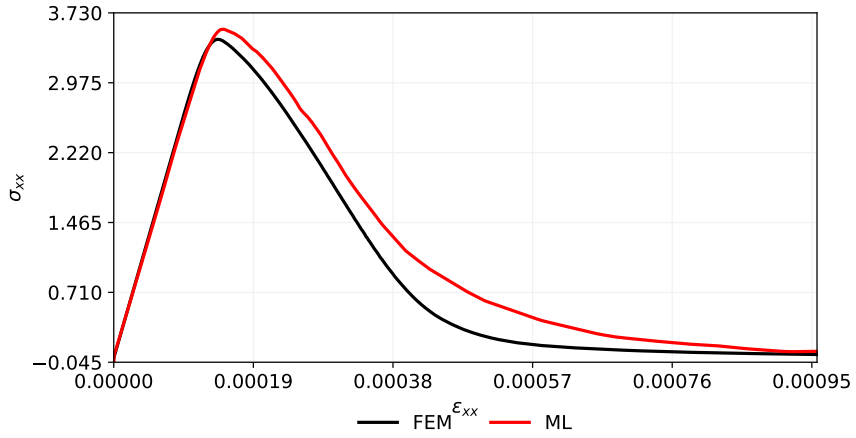

(a) Curve A (with smaller aggregates) and a $20\% fraction$

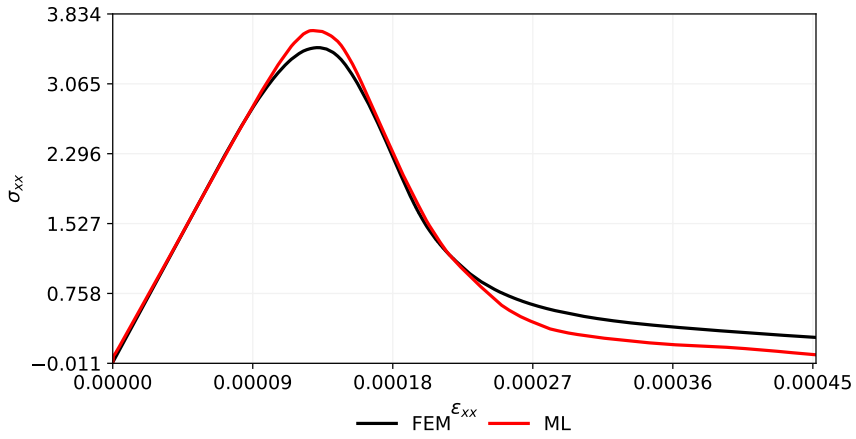

(b) Curve B (with medium aggregates) and a $30\% fraction$

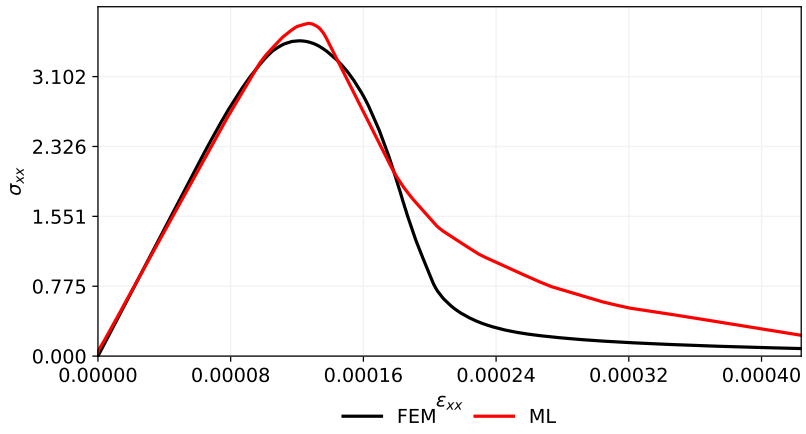

(c) Curve C (with bigger aggregates) and a $40\% fraction$

Figure 2. Comparison between the predictions of the ML model and the average curves of the simulated REVs.

The results obtained so far are promising. Although the predicted curves do not exactly align with the expected ones, the anticipated behavior is representative of the expected behavior for the RVE. The results presented here are preliminary, but it is anticipated that with a more robust database and more effective training, the deviation between the expected and predicted values will be significantly reduced. It is also important to note that with a well-trained machine learning model, the behavior of the RVE can be predicted using simple parameters, as the input variables were limited to characterizing the concrete composition in a straightforward manner and its state of deformation.

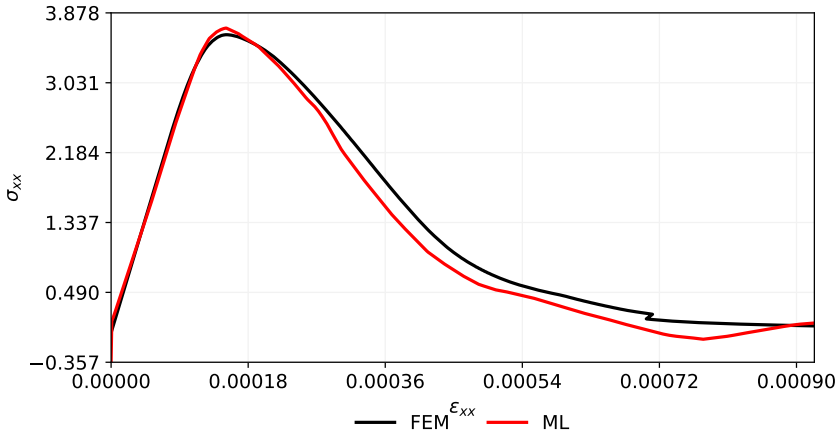

Figure 3. Curve A and a 27% fraction - A completely novel RVE for the ML model.

5 Conclusion

In conclusion, the current study demonstrates the potential of using machine learning models to predict the behavior of the RVE with considerable accuracy. The initial discrepancies observed between the predicted and expected curves highlight areas for further refinement, particularly in enhancing the database and optimizing the training process. Future work will focus on expanding the dataset and refining the machine learning algorithm to minimize prediction errors. This research underscores the feasibility of employing relatively simple input parameters to effectively model complex behaviors in solid mechanics, providing a foundation for more accurate and practical computational methods in the field.

Acknowledgements. The authors gratefully acknowledge the support from the Brazilian research agency CAPES and the contribution from the Insane Lab initiative with the computational environment for structural analysis used in the mechanical simulations presented in this research.

Authorship statement. The authors hereby confirm that they are the sole liable persons responsible for the authorship of this work, and that all material that has been herein included as part of the present paper is either the property (and authorship) of the authors, or has the permission of the owners to be included here.

References

[1] P. Trusov and I. Keller. The theory of constitutive relations. part i. *Perm State Technical University*, 1997.
[2] I. M. Gitman. *Representative Volumes and Multi-scale Modelling of Quasi-brittle Materials*. Inna M. Gitman, 2006.
[3] M. Ostoja-Starzewski, S. Kale, P. Karimi, A. Malyarenko, B. Raghavan, S. Ranganathan, and J. Zhang. Chapter two - scaling to rve in random media. volume 49 of *Advances in Applied Mechanics*, pp. 111 – 211. Elsevier, 2016.
[4] J. G. Van Mier. *Fracture processes of concrete*, volume 12. CRC press, 1996.
[5] Z. P. Bazant and D. Novak. Stochastic models for deformation and failure of quasibrittle structures: recent advances and new directions. *Computational modelling of concrete structures*, pp. 583–598, 2003.
[6] H. Tran and H. Chew. Cohesive zone interpretations of phase-field fracture models. *Journal of Applied Mechanics*, vol. 89, n. 12, pp. 121005, 2022.
[7] B. Bourdin, G. A. Francfort, and J.-J. Marigo. Numerical experiments in revisited brittle fracture. *Journal of the Mechanics and Physics of Solids*, vol. 48, n. 4, pp. 797–826, 2000.
[8] B. Bourdin and A. Chambolle. Implementation of an adaptive finite-element approximation of the mumford-shah functional. *Numerische Mathematik*, vol. 85, pp. 609–646, 2000.
[9] C. Kuhn, A. Schlüter, and R. Müller. On degradation functions in phase field fracture models. *Computational Materials Science*, vol. 108, pp. 374–384, 2015.
[10] A. Karma, D. A. Kessler, and H. Levine. Phase-field model of mode iii dynamic fracture. *Physical Review Letters*, vol. 87, n. 4, pp. 045501, 2001.

[11] M. J. Borden, T. J. Hughes, C. M. Landis, and C. V. Verhoosel. A higher-order phase-field model for brittle fracture: Formulation and analysis within the isogeometric analysis framework. *Computer Methods in Applied Mechanics and Engineering*, vol. 273, pp. 100–118, 2014.
[12] J. M. Sargado, E. Keilegavlen, I. Berre, and J. M. Nordbotten. High-accuracy phase-field models for brittle fracture based on a new family of degradation functions. *Journal of the Mechanics and Physics of Solids*, vol. 111, pp. 458–489, 2018.
[13] A. Khodadadian, N. Noii, M. Parvizi, M. Abbaszadeh, T. Wick, and C. Heitzinger. A bayesian estimation method for variational phase-field fracture problems. *Computational Mechanics*, vol. 66, pp. 827–849, 2020.
[14] T. T. Nguyen, J. Yvonnet, M. Bornert, C. Chateau, K. Sab, R. Romani, and R. Le Roy. On the choice of parameters in the phase field method for simulating crack initiation with experimental validation. *International Journal of Fracture*, vol. 197, pp. 213–226, 2016.
[15] E. Tanné, T. Li, B. Bourdin, J.-J. Marigo, and C. Maurini. Crack nucleation in variational phase-field models of brittle fracture. *Journal of the Mechanics and Physics of Solids*, vol. 110, pp. 80–99, 2018.
[16] H. M. Leao. A critical study on phse-field modelling of fracture. *Federal Univesity of Minas Gerais (UFMG)*, vol. , 2021.
[17] A. L. Samuel. Some studies in machine learning using the game of checkers. *IBM Journal of research and development*, vol. 3, n. 3, pp. 210–229, 1959.
[18] S. Haykin. *Neural networks: a comprehensive foundation*. Prentice Hall PTR, 1994.
[19] T. M. Mitchell and others. Machine learning, 1997.
[20] M. Awad and R. Khanna. *Machine Learning*, pp. 1–18. Apress, Berkeley, CA, 2015.
[21] I. Goodfellow, Y. Bengio, and A. Courville. *Deep learning*. MIT press, 2016.
[22] W. S. McCulloch and W. Pitts. A logical calculus of the ideas immanent in nervous activity. *The bulletin of mathematical biophysics*, vol. 5, pp. 115–133, 1943.
[23] F. Rosenblatt. The perceptron: a probabilistic model for information storage and organization in the brain. *Psychological review*, vol. 65, n. 6, pp. 386, 1958.
[24] D. E. Rumelhart, G. E. Hinton, and R. J. Williams. Learning representations by back-propagating errors. *nature*, vol. 323, n. 6088, pp. 533–536, 1986.
[25] Z. Wang, A. Kwan, and H. Chan. Mesoscopic study of concrete i: generation of random aggregate structure and finite element mesh. *Computers and Structures*, vol. 70, n. 5, pp. 533–544, 1999.